

## ORIGINAL RESEARCH

Engulfment and Cell Motility Protein 1 (ELMO1) Has an Essential Role in the Internalization of *Salmonella* Typhimurium Into Enteric Macrophages That Impact Disease Outcome

Soumita Das,<sup>1</sup> Arup Sarkar,<sup>2</sup> Sarmistha Sinha Choudhury,<sup>1</sup> Katherine A. Owen,<sup>3</sup> Victoria L. Derr-Castillo,<sup>1</sup> Sarah Fox,<sup>1</sup> Lars Eckmann,<sup>4</sup> Michael R. Elliott,<sup>5</sup> James E. Casanova,<sup>3</sup> and Peter B. Ernst<sup>1</sup>

<sup>1</sup>Department of Pathology, University of California San Diego, San Diego, California; <sup>2</sup>Trident School of Biotech Sciences, Trident Academy of Creative Technology, Odisha, India; <sup>3</sup>Department of Cell Biology, University of Virginia, Charlottesville, Virginia; <sup>4</sup>Department of Medicine, University of California San Diego, San Diego, California; <sup>5</sup>Department of Microbiology and Immunology, University of Rochester School of Medicine, Rochester, New York

## SUMMARY

ELMO1, involved in internalization of *Salmonella* in intestinal phagocytes with less bacterial dissemination and inflammation in ELMO1 knockout mice, activates Ras-related C3 botulinum toxin substrate 1 (Rac1) and inflammatory signals, increasing tumor necrosis factor- $\alpha$  with enteric infection and inflammatory diseases.

**CONCLUSIONS:** These findings suggest a novel role for ELMO1 in facilitating intracellular bacterial sensing and the induction of inflammatory responses after infection with *Salmonella*. (*Cell Mol Gastroenterol Hepatol* 2015;1:311–324; <http://dx.doi.org/10.1016/j.jcmgh.2015.02.003>)

**Keywords:** Engulfment Pathway; Enteric Infection; Host Cellular Responses; Intestinal Inflammation; *Salmonella*.

**BACKGROUND & AIMS:** After invading intestinal epithelial cells, enteric bacteria encounter phagocytes, but little is known about how phagocytes internalize the bacteria to generate host responses. BAI1 (brain angiogenesis inhibitor 1) binds and internalizes Gram-negative bacteria through an engulfment and cell motility protein 1 (ELMO1)/Ras-related C3 botulinum toxin substrate 1 (Rac1)-dependent mechanism. We delineate the role of ELMO1 in host inflammatory responses after enteric infection.

**METHODS:** ELMO1-depleted murine macrophage cell lines, intestinal macrophages, and ELMO1-deficient mice (total or myeloid-cell specific) were infected with *Salmonella enterica* serovar Typhimurium. The bacterial load, inflammatory cytokines, and histopathology were evaluated in the ileum, cecum, and spleen. The ELMO1-dependent host cytokines were detected by a cytokine array. ELMO1-mediated Rac1 activity was measured by pull-down assay.

**RESULTS:** The cytokine array showed a reduced release of proinflammatory cytokines, including tumor necrosis factor- $\alpha$  (TNF- $\alpha$ ) and monocyte chemoattractant protein 1 (MCP-1), by ELMO1-depleted macrophages. Inhibition of ELMO1 expression in macrophages decreased Rac1 activation (~6-fold) and reduced internalization of *Salmonella*. ELMO1-dependent internalization was indispensable for TNF- $\alpha$  and MCP-1. Simultaneous inhibition of ELMO1 and Rac function virtually abrogated TNF- $\alpha$  responses to infection. Activation of nuclear factor  $\kappa$ B, extracellular signal-regulated kinases 1/2, and p38 mitogen-activated protein kinases were impaired in ELMO1-depleted cells. Bacterial internalization by intestinal macrophages completely depended on ELMO1. *Salmonella* infection of ELMO1-deficient mice resulted in a 90% reduction in bacterial burden and attenuated inflammatory responses in the ileum, spleen, and cecum.

Each year 4 to 6 million people die of enteric infections. *Salmonella enterica* is the second leading cause of enteric infections, contributing to significant morbidity and mortality.<sup>1</sup> Once ingested, *Salmonella* enters the intestinal epithelial cells via bacteria-mediated invasion mechanisms; subsequently, the organisms encounter phagocytes, including macrophages, in the lamina propria.<sup>1,2</sup> Subsequent to the engulfment of pathogenic bacteria, macrophages initiate inflammatory responses that eventually transition to adaptive immunity. To date, a great deal of research has focused on the contribution of epithelial cells to the pathogenesis of *Salmonella* infection, but the

**Abbreviations used in this paper:** BAI, brain angiogenesis inhibitor; BAY 11-7082, (E)-3-(4-methylphenyl)sulfonylprop-2-enitrile; BMDM, bone marrow-derived macrophages; Dock180, dedicator of cytokinesis 180; ELISA, enzyme-linked immunosorbent assay; ELMO1, engulfment and cell motility protein 1; ERK<sub>1/2</sub>, extracellular signal-regulated kinases 1/2; GST, glutathione S-transferase; GTP, guanosine triphosphate; JNK, c-Jun N-terminal kinase; KO, knockout; LPS, lipopolysaccharide; MAPK, mitogen-activated protein kinase; MCP-1, monocyte chemoattractant protein 1; moi, multiplicity of infection; NF- $\kappa$ B, nuclear factor  $\kappa$ B; PAMP, pathogen-associated molecular pattern; PBD, p21-binding domain of Pak1; PBS, phosphate-buffered saline; PD98059, 2-(2-amino-3-methoxyphenyl)-4H-1-benzopyran-4-one; PRR, pattern recognition receptor; Rac1, Ras-related C3 botulinum toxin substrate 1; RANTES, regulated on activation normal T-cell expressed and secreted; RT-PCR, reverse-transcription polymerase chain reaction; SB203580, 4-(4-fluorophenyl)-2-(4-methylsulfinylphenyl)-5-(4-pyridyl)1H-imidazole; shRNA, small-hairpin RNA; SPI, *Salmonella* pathogenicity island; TLR, Toll-like receptor; TNF- $\alpha$ , tumor necrosis factor- $\alpha$ ; U0126, 1,4-diamino-2,3-dicyano-1,4-bis(methylthio)butadiene; WT, wild type.

© 2015 The Authors. Published by Elsevier Inc. on behalf of the AGA Institute. This is an open access article under the CC BY-NC-ND license (<http://creativecommons.org/licenses/by-nc-nd/4.0/>).

2352-345X

<http://dx.doi.org/10.1016/j.jcmgh.2015.02.003>

involvement of the phagocytic cells in the induction of inflammation has been less studied.

Bacteria interact with host cells via multiple pattern recognition receptors (PRRs) that recognize microbial products or pathogen-associated molecular patterns (PAMPs).<sup>3</sup> Many studies have investigated the signaling and host responses triggered by receptors such as Toll-like receptor 4 (TLR4). TLR4 binds bacterial lipopolysaccharide (LPS) with the help of CD14 and MD2. Many studies have used in vitro endotoxin concentrations ranging from 100 ng/mL to 1  $\mu$ g/mL, levels that would mimic an encounter with millions of bacteria per cell. In contrast, disease occurs with far fewer bacterial interactions, suggesting that phagocytosed bacteria provide a more efficient means to deliver a signal to PRRs. Thus, we examined the role of the host engulfment pathway in phagocytes and the subsequent inflammatory responses.

We previously had identified brain angiogenesis inhibitor 1 (BAI1) as a pattern recognition receptor that recognizes the core carbohydrate of LPS, distinct from TLR4 which binds the lipid A part of LPS. The intracellular domain of BAI1 interacts with engulfment and cell motility protein 1 (ELMO1) and dedicator of cytokinesis 180 (Dock180) to act as a bipartite guanine nucleotide exchange factor for the small Rho GTPase Ras-related C3 botulinum toxin substrate 1 (Rac1).<sup>4,5</sup> Subsequently, activated Rac1 facilitates the engulfment of the bound cargo.<sup>6</sup> The importance of Rac1 in *Salmonella*-mediated bacterial inflammatory responses in epithelial cells was established previously.<sup>7</sup> Our present study addresses the contribution of ELMO1-mediated Rac activation, bacterial engulfment by phagocytes, including intestinal macrophages, and the subsequent induction of inflammatory responses.

We found that internalization of bacteria not only contributes to the maximal cytokine production but that ELMO1 and Rac1 collectively are required for both internalization and proinflammatory responses. The relevance of this pathway became evident when intestinal macrophages isolated from ELMO1 knockout (KO) mice failed to internalize *Salmonella*, and infection of these mice led to a lower bacterial load in the ileum and spleen and attenuated tumor necrosis factor- $\alpha$  (TNF- $\alpha$ ) and monocyte chemoattractant protein 1 (MCP-1) responses compared with wild-type (WT) mice. Similarly, LysM cre mice devoid of ELMO1 in myeloid cells had lower bacterial loads and reduced TNF- $\alpha$  responses, indicating the importance of the ELMO1 pathway in phagocytes and the induction of host inflammatory responses. These studies suggest that the ELMO1 pathway has an important role in the contribution of phagocytes to the pathogenesis of disease after enteric infection with *Salmonella*.

## Materials and Methods

### Bacteria

*Salmonella enterica* serovar Typhimurium strain SL1344 were obtained from the American Type Culture Collection (Manassas, VA) and were maintained as described previously elsewhere.<sup>4</sup> For bacterial culture, a single colony was

inoculated into Luria-Bertani broth and grown for 8 hours under aerobic conditions in an orbital shaking incubator at 150 rpm and then under oxygen-limiting conditions overnight to maintain their invasiveness.<sup>8</sup> The expression of *Salmonella* pathogenicity island (SPI-1 and SPI-2) genes was tested and compared with the bacteria grown under low and high salt concentrations for their optimal expression. Under these conditions, the bacteria corresponded to  $5\text{--}7 \times 10^8$  colony forming units. The cells were infected at a multiplicity of infection (moi) of 10 unless otherwise indicated.

### Mice

We purchased C57 BL/6 mice from the Jackson Laboratory (Bar Harbor, ME). ELMO1 KO mice and LysM<sup>cre+</sup> ELMO1<sup>fl/fl</sup> mice were generated as described previously elsewhere<sup>9</sup> and were bred at the University of California–San Diego by mating heterozygotic breeders to yield offspring with various degrees of ELMO1 expression but shared exposure to the environmental microbiota during their rearing. The Institutional Animal Care and Use Committee at the University of California–San Diego approved all animal experiments, and efforts were made to minimize animal suffering during the study.

### Cell Lines

Control or ELMO1 small-hairpin RNA (shRNA) J774 cells were maintained in high glucose Dulbecco's modified Eagle's medium containing 10% fetal calf serum, 2 mM L-glutamine, 1 mM sodium pyruvate, 4.5 g/liter glucose, and antibiotics in a 5% CO<sub>2</sub> incubator at 37°C. Cells were transfected using Lipofectamine 2000 (Invitrogen/Life Technologies, Carlsbad, CA) as described previously elsewhere.<sup>4</sup>

### Down-Regulation of ELMO1

ELMO1 was stably down-regulated using a shRNA construct, as described previously elsewhere<sup>5</sup> (with a sequence within the exon GCAGAGTCAGAACCTAATA). ELMO1, ELMO2, and Rac1 was transiently down-regulated in bone-marrow-derived macrophage (BMDM) cells by nucleofection with ON-Target Plus SMART pool siRNA from Dharmacon (GE Healthcare, Lafayette, CO) using the Amara mouse macrophage nucleofector kit program Y-001 (Lonza, Cologne, Germany). After 48 hours, the RNA was prepared to monitor the level of ELMO1 or ELMO2 or Rac1 expression by real-time reverse-transcription polymerase chain reaction (RT-PCR).

### Bacterial Binding and Internalization

For bacterial binding, the cells were treated with cytochalasin D (1  $\mu$ M) to block bacterial entry. Quantification of intracellular bacteria was performed using the gentamicin protection assay.<sup>4</sup> Approximately  $2 \times 10^5$  cells/well were seeded into 24-well culture dishes 18 hours before infection at a moi of 10 for 1 hours in antibiotic-free media. The cells were then washed and incubated with gentamicin (500  $\mu$ g/mL) for 90 minutes to kill the extracellular bacteria. Subsequently, the cells were lysed in 1% Triton-X 100, and

the lysates were serially diluted and plated directly onto Luria-Bertani agar plates. The total colony-forming units were enumerated the next day after overnight incubation at 37°C.

### **Bone Marrow–Derived Macrophages Preparation**

Primary bone marrow–derived macrophages (BMDM) were derived from the femurs and tibia of mice using techniques described previously elsewhere.<sup>29</sup> The marrow was flushed from mouse leg bones with medium (RPMI + 10% fetal calf serum supplemented with 2 mM glutamine, 1 mM sodium pyruvate) and seeded onto Petri dishes. For growth of bone marrow macrophages, RPMI medium was supplemented with 20% of supernatant taken from L929 cells (containing murine granulocyte–macrophage colony stimulating factor, referred to as BMDM medium).

### **Isolation of Intestinal Macrophages**

Gut antigen presenting cells were isolated using techniques described previously elsewhere.<sup>4</sup> Briefly, small intestines were removed, opened longitudinally to flush out feces, cut into 15-mm pieces, and then incubated for 20 minutes at 37°C on a shaker in Hank's balanced salt solution supplemented with 5% heat-inactivated fetal bovine serum and 2 mM EDTA. After passing the preparation through a metal filter, the intestinal fragments were collected, and the step was repeated. Subsequently, intestinal fragments were minced and incubated for 20 minutes at 37°C on a shaker in Hank's balanced salt solution supplemented with 5% heat-inactivated fetal bovine serum and 1 mg/mL type VIII collagenase (Sigma-Aldrich, St. Louis, MO). The cell suspension was passed through a cell strainer to remove debris, washed, and then the CD11b<sup>+</sup> cells were enriched with a CD11b MACS kit (Miltenyi Biotec, Bergisch Gladbach, Germany). In some instances, intestinal macrophages were labeled using monoclonal antibody CD11b (BD Biosciences, San Jose, CA) and sorted using a FACS Vantage (BD Biosciences). The percentage of macrophages in cell population was examined by staining with antibody specific for the macrophage marker F4/80.

### **Rac Activity Assay**

Rac1 activity was assayed by pull-down assay using GST-PBD (glutathione *S*-transferase with p21-binding domain of Pak1) beads as described previously elsewhere.<sup>4</sup> Infected cells were lysed in buffer containing 50 mM Tris-HCl (pH 7.5), 2 mM MgCl<sub>2</sub>, 0.1 M NaCl, 1% NP-40, and 10% glycerol with protease inhibitors and incubated with GST coupled to PBD to precipitate Rac-GTP. The blots were visualized using Pierce SuperSignal electrochemiluminescence reagents. The ratio of active Rac1 (GTP bound) to total Rac1 was quantified using Image Quant 5.2 (Molecular Dynamics, Sunnyvale, CA).

### **Cytokine Assays**

A proteome profiler array (mouse cytokine array panel A; R&D Systems, Minneapolis, MN) was used to assay the level of 40 cytokines according to the manufacturer's

instructions. Briefly, the capture antibody of cytokines and chemokines were spotted on nitrocellulose membranes. The sample/antibody mixture was incubated, and the cytokine-chemokine antibody complex was bound to the immobilized capture antibody on the membrane. After the streptavidin-horseradish peroxidase and chemiluminescent reagents had been added, the signal was proportional to the amount of cytokine bound. For secreted cytokines, supernatants were collected from infected/treated cells at the indicated times. Mouse TNF- $\alpha$  (BD Biosciences/Pharmin-gen) and mouse MCP-1 (R&D Biosystems) were measured using an enzyme-linked immunosorbent assay (ELISA) kit according to the manufacturer's instructions.

### **Assessment of Cellular Signaling**

We plated  $5 \times 10^6$  cells in a 10-cm dish 20 hours before the experiment. After adherence of the cells, we replaced the medium, and the cells were serum starved for 16 hours. After the indicated time of infection, the cells were washed twice with cold phosphate-buffered saline (PBS) and lysed using modified radioimmunoprecipitation assay buffer (50 mM Tris [pH 7.4], 150 mM NaCl, 1% NP-40, 0.25% N-deoxycholate, 1 mM EDTA with protease inhibitor cocktail [Sigma-Aldrich], and Halt phosphatase inhibitor cocktail [Thermo Fisher Scientific, Waltham, MA]). Approximately, 50  $\mu$ g of protein was loaded on 10%–15% sodium dodecyl sulfate-polyacrylamide gels, depending on the size of the protein, and the protein was probed using the indicated antibodies.

Western blot analyses were performed using the following antibodies: total extracellular signal-regulated kinases 1/2 (ERK<sub>1/2</sub>), phospho-ERK<sub>1/2</sub>, total p38, phospho-p38, total c-Jun *N*-terminal kinase (JNK), phospho-JNK, total p65, phospho-p65, and phospho-I $\kappa$ B $\alpha$  were purchased from Cell Signaling Technology (Beverly, MA).

### **Infection of Mice**

To assess the role of ELMO1 after bacterial infection *in vivo*, age- and gender-matched ELMO1 KO mice and WT C57BL/6 mice were infected with 10<sup>8</sup> *Salmonella enterica* serovar Typhimurium SL1344 by gavage. This model was selected in preference to the streptomycin pretreated colitis model where antibiotic treatment can alter the microbial composition. During the infection period, the mice were monitored for weight and clinical signs of disease. At day 5 after infection, the mice were killed and their tissues collected to assess bacterial burden, pathology, and cytokine responses.

### **Histopathology**

The cecum and ileum were fixed in 10% neutral buffered formalin, processed according to standard procedures for paraffin embedding, cut into 5- $\mu$ m sections in the University of California–San Diego histopathology core and stained with H&E. The pathology score of cecal sections was determined by blinded examination by a veterinary pathologist (V.C.). Each section was evaluated for the presence of neutrophils, mononuclear infiltrates, submucosal

edema, surface erosions, inflammatory exudates, and the presence of crypt abscesses. A scoring system was developed (as described in Table 1) based on a modification of previously published techniques<sup>10,11</sup> for the quantitative analysis of cecal inflammation. The total score was calculated as the sum of the individual parameters.

### RNA Preparation, Real-Time Reverse-Transcription Polymerase Chain Reaction

Total RNA was extracted using the RNeasy kit (Qiagen, Valencia, CA) and was reverse transcribed with a Superscript kit (Invitrogen/Life Technologies), both according to the manufacturer's instructions. Real-time RT-PCR was performed using Taqman gene expression assays with FAM-labeled primer/probes (Applied Biosystems, Foster City, CA) detected in a SmartCycler (Cepheid, Sunnyvale, CA) and normalized to the 18S rRNA signal. The fold change in the mRNA expression was determined using the  $\Delta\Delta C_t$  method.<sup>12</sup>

### Confocal Microscopy

Control and ELMO1 shRNA (J774) cells were infected with RFP-labeled *Salmonella* (SL1344-RFP) for 5 minutes at a moi of 10. Samples were washed in 1X PBS, pH 7.4 and fixed in 2% formaldehyde, washed with PBS, and permeabilized with 0.1% triton in PBS for 5 minutes. Cells were blocked with 5% goat serum -1.5% bovine serum albumin in PBS (blocking solution) and subsequently incubated with Alexa 488 Phalloidin (Life Technologies) to stain F-actin (green).

The cells were washed and incubated for 5 minutes in Hoechst 33342 (Life Technologies) diluted 1:2000 in 1X PBS to stain the nuclei. The cells were washed with 1X PBS and subsequently mounted on glass slides with prolong gold. Confocal images were obtained with a 100 $\times$  objective using an Olympus FV1000 Confocal microscope system (Olympus America, Center Valley, PA).

### Statistical Analysis

Bacterial internalization and ELISA results were expressed as the mean  $\pm$  standard deviation and compared

using a two-tailed Student *t* test.  $P < .05$  was considered statistically significant. For animal experiments, each point represents a single mouse, and the median indicated as described. Data were compared using a Mann-Whitney *U* test by the GraphPad biostatistics package (GraphPad Software, San Diego, CA).  $P < .05$  was considered statistically significant.

## Results

### ELMO1 Promotes Bacterial Internalization Into Macrophages

To understand the role of ELMO1 in bacterial internalization, ELMO1 expression was stably inhibited in the murine macrophage cell line J774 using ELMO1 shRNA. ELMO1 expression was approximately 90% lower (Figure 1A). The contribution of ELMO1 to the internalization of *Salmonella* was assessed in ELMO1 shRNA cells using the gentamicin protection assay. This approach showed that internalization of *Salmonella* was impaired by approximately 50% (Figure 1B).

To address the role of ELMO1 in bacterial internalization in a more physiologically relevant system, intestinal macrophages enriched from wild type (WT) or ELMO1 KO mice were infected. Binding of bacteria in the presence of cytochalasin D was comparable between macrophages from both WT and ELMO1 KO mice. Whereas internalization by gentamicin protection assay was ablated in macrophages from ELMO1 KO mice, intestinal macrophages from WT mice engulfed the bacteria efficiently. The dependence on ELMO1 for bacterial internalization was independent of their ability to bind as the macrophages from both WT and ELMO1 KO mice bound *Salmonella* comparably (see Figure 1C). The involvement of ELMO1 in bacterial internalization is consistent with the fact that ELMO1 is the cytosolic protein that interacts with the cytoplasmic portion of the BAI1 receptor that binds Gram-negative bacteria.<sup>4</sup>

Bacterial internalization was also tested in BMDM isolated from WT and ELMO1 KO mice. Internalization of bacteria was comparable in BMDM from WT and ELMO1 KO mice (Figure 2A). Because ELMO2 expression was higher in the BMDM from ELMO1 KO mice, it may have compensated

**Table 1.** Criteria for scoring histological inflammation

Parameter	Score			
	0	1	2	3
Thickness	<350 $\mu\text{m}$	350–499 $\mu\text{m}$	500–750 $\mu\text{m}$	>750 $\mu\text{m}$
Mononuclear infiltrate	Small numbers of lymphocytes; rare intraepithelial lymphocytes	Mild multifocal small aggregates within the superficial mucosa	Multifocal (>5) to regionally extensive infiltrate, extends to submucosa (spans <3 crypt lengths)	Regionally extensive, replaces crypts, spans >3 crypt lengths
PMN infiltrate	Rare neutrophils <3 PMN/40 $\times$ field	<10 PMN/40 $\times$ field; intraepithelial PMN	Multifocal aggregates 10–30 PMN/40 $\times$ field $\pm$ crypt abscess	Diffuse aggregates; >30 PMN/40 $\times$ field + crypt abscesses
Extent of inflammation		Mucosal	Mucosal + Submucosal	Transmural

Note: PMN, polymorphonuclear neutrophil.



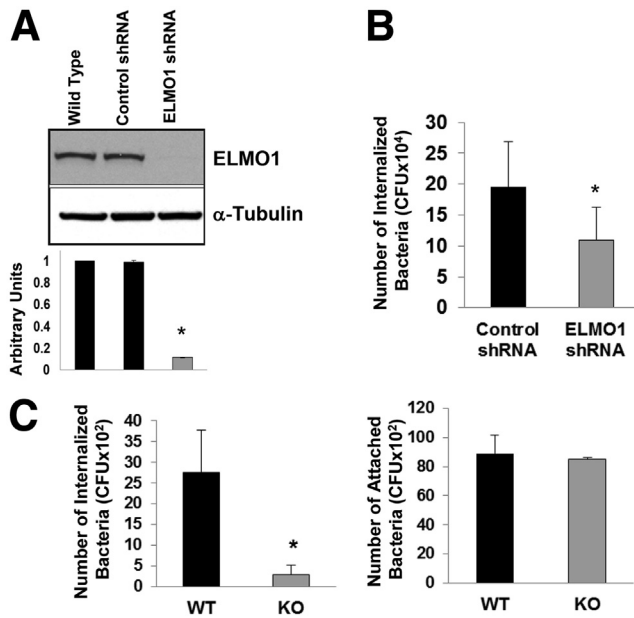


**Figure 1. Engulfment and cell motility protein 1 (ELMO1) regulates bacterial internalization.** (A) ELMO1 expression assayed in control small-hairpin RNA (shRNA) and the ELMO1 shRNA J774 cells. The upper panel is the Western blot from one representative experiment. The lower panel is the densitometry of the bands from three separate experiments where arbitrary units were represented by the ratio of ELMO1 to  $\alpha$ -tubulin. Data represent the mean  $\pm$  standard deviation (SD) of three separate experiments. (B) Control and ELMO1 shRNA cells or (C) intestinal macrophages isolated from wild type (WT) and ELMO1 knockout mice (KO) incubated with *Salmonella enterica* serovar Typhimurium (SL1344) for 1 hour at 37°C, with internalization measured as described in *Materials and Methods* using a gentamicin protection assay. The binding of *Salmonella* was determined in intestinal macrophages isolated from WT and ELMO1 KO mice in the presence of cytochalasin D to block internalization. In B the average number of internalized bacteria (mean  $\pm$  SD) was calculated from five separate experiments. In C the average number (mean  $\pm$  SD) of internalized bacteria (*left*) and attached bacteria (*right*) was calculated from three separate experiments. \* $P \leq .05$ , two-tailed Student *t* test.

for the absence ELMO1 (see [Figure 2B](#)). We found that in BMDM the individual siRNA could inhibit ELMO1 and ELMO2 expression approximately 80% as assessed by real-time RT-PCR (data not shown). When we used these cells, bacterial internalization was decreased 50% and 30% in the ELMO1- and ELMO2-siRNA treatments, respectively (see [Figure 2C](#)), suggesting that ELMO2 can compensate the effect of bacterial internalization in BMDM isolated from ELMO1 KO mice.

Interestingly, in intestinal macrophages, the compensatory effect of ELMO2 was not observed even though it was expressed but not up-regulated compared with the cells from WT mice (see [Figure 2B](#)). A compensatory effect of ELMO2 also was not observed in the ELMO1 shRNA cells generated in the J774 cell line (data not shown). The inhibition of Rac1 decreased bacterial internalization in the control and ELMO1 shRNA cells (see [Figure 2D](#)).

### ELMO1-Mediated Rac1 Activation Regulates Proinflammatory Cytokine Production in Response to Infection

During apoptotic cell recognition and engulfment; ELMO1/Dock 180 catalyzes the loading of inactive (GDP-bound) Rac1 with GTP.<sup>6</sup> To confirm that Rac1 was activated in an ELMO1-dependent manner after infection, the J774 cells or cells depleted of ELMO1 by shRNA were infected with *Salmonella*, and the activation of Rac1 was assessed ([Figure 3A](#)). In control cells, active Rac1 increased starting at 15 minutes after infection. Rac1 was maximally activated 1 hour after infection in control shRNA cells, reaching levels nearly 4-fold greater than the uninfected controls. In contrast, the basal level of Rac1 activity failed to increase in response to *Salmonella* infection in cells depleted of endogenous ELMO1. At 1 hour after infection, the Rac1 activity was 6-fold less in ELMO1 shRNA cells compared with control cells. Thus, the optimal activation of Rac1 by *Salmonella* in cultured macrophages requires ELMO1 (see [Figure 3A](#)). Rac1 shares 92% identical amino acids with Rac2. Probing the same pull-down material with a Rac2-specific antibody showed no Rac2 activity in J774 cells after infection (data not shown), which suggests that the ELMO1/Dock180 complex does not appreciably activate Rac2.

If cytokine production in infection requires internalization, we predicted that host responses would be dependent on the engulfment mediated through the ELMO1/Rac1 pathway. To determine whether ELMO1 regulated inflammatory cytokines induced by infection, multiple cytokines/chemokines were assayed using a proteome profiler cytokine array (see [Figure 3B](#)). Granulocyte-colony stimulating factor, MCP-1, TNF- $\alpha$ , keratinocyte-derived chemokine, and regulated on activation normal T-cell expressed and secreted (RANTES) were all higher in the *Salmonella*-infected control shRNA cells compared with the ELMO1 shRNA cells (as shown in [Figure 3B](#)).

TNF- $\alpha$  is a major contributing proinflammatory cytokine early in the pathogenesis of *Salmonella*<sup>13</sup> as well as in the transition to host protection.<sup>14</sup> Because ELMO1/Dock 180 activates Rac1, we investigated the role of Rac1 in the production of TNF- $\alpha$  by both inhibiting Rac1 in control shRNA cells or complementing ELMO1 shRNA cells with a constitutively active form of Rac (Rac-V12, the active form of Rac). Treatment of shRNA cells with a small molecule inhibitor of Rac (NSC23766) reduced TNF- $\alpha$  responses more than 75%. Furthermore, inhibition of Rac in the ELMO1 shRNA cells almost ablated the TNF- $\alpha$  response (see [Figure 3C](#)). When ELMO1 shRNA cells were transfected with the Rac-V12, TNF- $\alpha$  production was restored to levels detected in the control shRNA cells. Further, transfection of the control shRNA cells with Rac-V12 led to a twofold increase in TNF- $\alpha$  production in response to infection with *Salmonella*.

The inhibition of Rac1 decreased bacterial internalization in control and ELMO1 shRNA cells, and that in turn regulated cytokine responses. To demonstrate further that internalized bacteria promote cytokine responses, control and ELMO1 shRNA cells were treated with cytochalasin D to

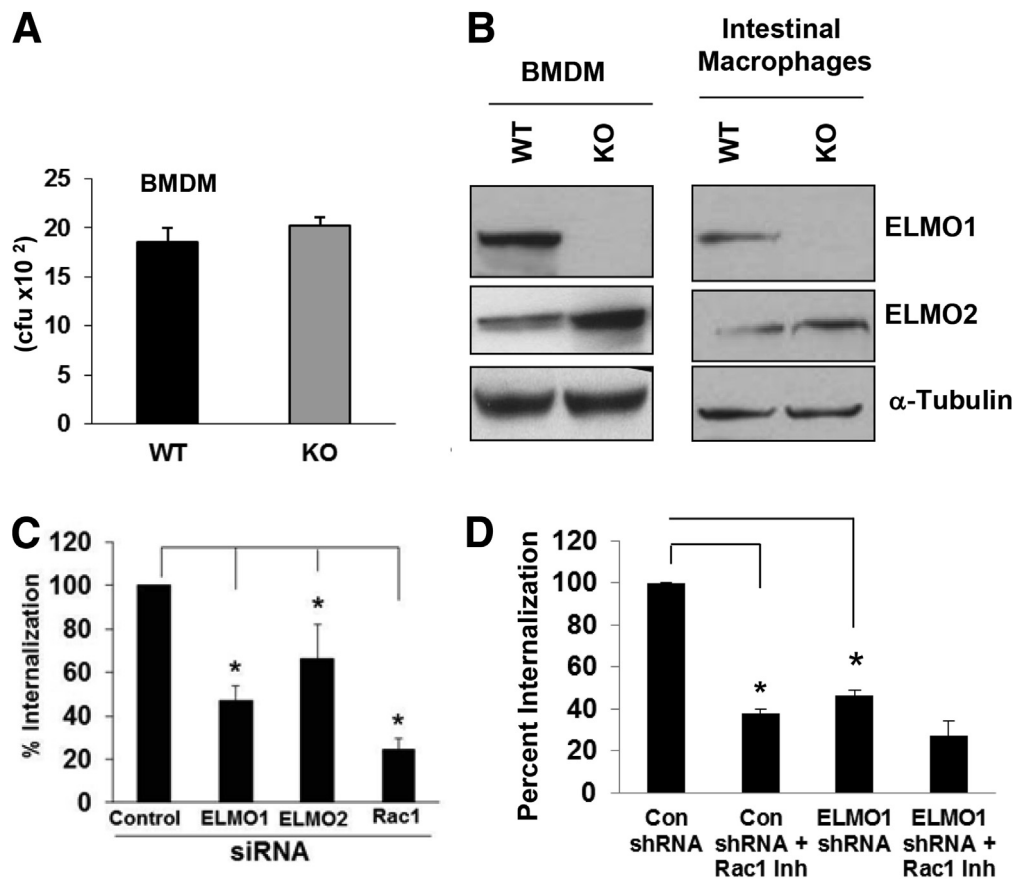


**Figure 2.** Engulfment and cell motility protein 1 (ELMO1), ELMO2, and Ras-related C3 botulinum toxin substrate 1 (Rac1) regulates bacterial internalization in bone marrow-derived macrophages (BMDM). (A) Bone marrow-derived macrophages BMDM from wild-type (WT) and ELMO1 knockout (KO) mice infected with *Salmonella enterica* serovar Typhimurium SL1344. After 1 hour of infection, the internalization was measured as described in *Materials and Methods* using a gentamicin protection assay. Data are presented as the percentage of internalization from three independent experiments. (B) Expression of ELMO1 and ELMO2 detected in cell lysates isolated from BMDM and intestinal macrophages isolated from WT and ELMO1 KO mice. In the lower panel,  $\alpha$ -tubulin was used as a loading control. (C) Internalization of *Salmonella* measured in control, ELMO1, ELMO2, or Rac1 small-interfering RNA-treated cells from BMDM isolated from WT BL/6 mice. Internalization was measured after 1 hour of infection, same as in A. Data are presented as the percentage of internalization from three independent experiments. \* $P \leq .05$ , as assayed by two-tailed Student's *t* test. (D) Internalization of *Salmonella* measured in control and ELMO1 small-hairpin RNA (shRNA) cells (J774) in the presence or absence of Rac1 inhibitor. Internalization was measured after 1 hour of infection, same as in A. Data are presented as the percentage of internalization from three independent experiments. \* $P \leq .05$ , two-tailed Student *t* test.

prevent bacterial entry. Figure 3E showed that cytochalasin D inhibited TNF- $\alpha$  at a comparable level in control and ELMO1 shRNA cells indicating the ELMO1-mediated internalization regulates cytokine responses.

Monocyte chemo attractant protein 1 (CCL2 or MCP-1) is important for the survival of mice during *Salmonella* infections and promotes bacterial killing by macrophages.<sup>15,16</sup> Because the cytokine array implicated a role for ELMO1 in the control of MCP-1, we validated the MCP-1 responses by ELISA. The ELMO1 shRNA cells showed a decrease in MCP-1 compared with the control shRNA cells (see Figure 3F). Interestingly, in control and ELMO1 shRNA cells after infection, treatment with the Rac1 inhibitor decreased the MCP-1 level, and cytochalasin D treatment resulted in a dramatic reduction in the MCP-1 response.

BAI1 binds bacterial LPS of Gram-negative bacteria irrespective of their pathogenic status. To determine the

effect of LPS and other PAMPS such as TLR2 ligand, we tested lipoteichoic acid and the TLR4 ligand Lipid A in the production of ELMO1-mediated TNF- $\alpha$  (see Figure 3G). After 3 hours of treatment, the parental J774 cells, control, and ELMO1 shRNA cells showed comparable levels of TNF- $\alpha$ , again supporting the notion that the responses induced by infection were mediated subsequent to internalization.

### ELMO1 Regulates NF- $\kappa$ B and MAP Kinase Activation

The expression of several inflammatory cytokines is regulated through the mitogen-activated protein kinase (MAPK) pathway and/or nuclear factor  $\kappa$ B (NF- $\kappa$ B) signaling.<sup>17,18</sup> Therefore, we examined the activation of these pathways in control and ELMO1 shRNA cells after infection with *Salmonella*. Levels of phospho-I $\kappa$ B were decreased in

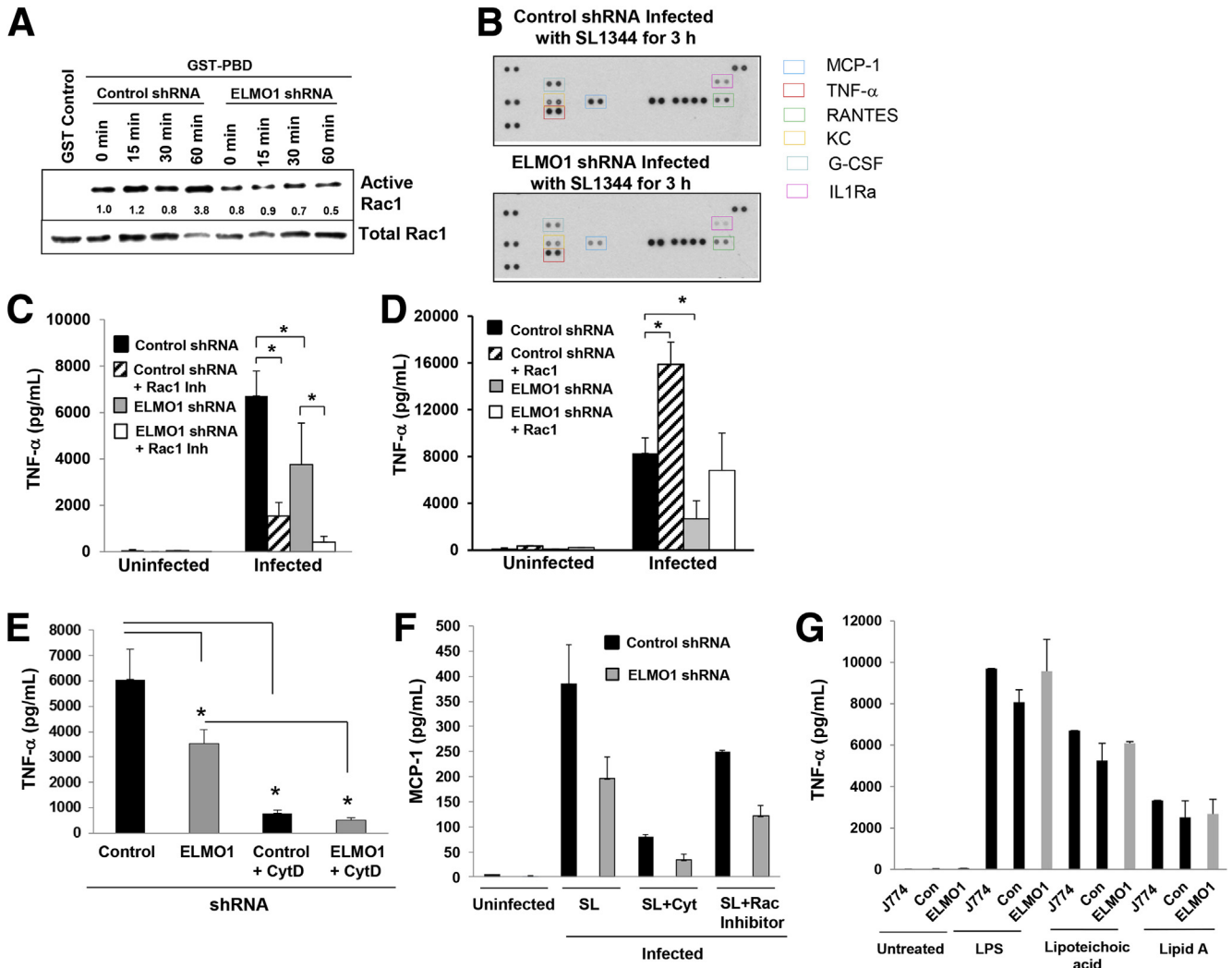


**Figure 3. Maximal tumor necrosis factor- $\alpha$  (TNF- $\alpha$ ) responses after *Salmonella* infection require engulfment and cell motility protein 1 (ELMO1)-mediated Ras-related C3 botulinum toxin substrate 1 (Rac1) activation.** (A) Guanosine triphosphate (GTP)-bound Rac1 affinity purified from cell lysates with glutathione S-transferase (GST) alone as a negative control (lane 1) or GST-PBD [p21-binding domain of p21-activated kinase 1 or PAK1]. The pull-down is based on the fact that only the GTP-bound active form binds GST-PBD whereas the GDP bound inactive Rac1 does not. Control and ELMO1 small-hairpin RNA (shRNA) J774 cells were infected with SL1344 at a multiplicity of infection of 10 for the indicated times and lysed. Pull-downs (upper panel) and a fraction of the lysate (middle panel) were simultaneously blotted for Rac1. The ratio of GTP-bound to total Rac1 corrected for total protein is expressed relative to uninfected cells (lane 2). (B) Proteome profiler array panel comparing the expression of cytokines and chemokines in the supernatant from control and ELMO1 shRNA cells for 3 hours after infection with *Salmonella* SL1344. A representative blot was shown from three different experiments in. In the right side, the colored boxes indicate the list of cytokines that were highlighted twofold or more in the blot. (C) TNF- $\alpha$  enzyme-linked immunosorbent assay (ELISA) performed from control or ELMO1 shRNA cells (J774) after 3 hours of infection with *Salmonella* (SL1344) in the presence or absence of the Rac1 inhibitor (NSC23766; 50  $\mu$ M). (D) Control and ELMO1 shRNA cells (J774) transfected with an active form of Rac1 (V12). Subsequently, the TNF- $\alpha$  production was assessed by ELISA from uninfected and SL1344 infected cells 3 hours after infection. (E) TNF- $\alpha$  ELISA performed from control and ELMO1 shRNA cells (J774) after 3 hours of infection with *Salmonella* (SL1344) in the presence or absence of cytochalasin D. (F) Monocyte chemoattractant protein 1 (MCP-1) ELISA performed from control and ELMO1 shRNA cells (J774) either uninfected or after 3 hours of infection with *Salmonella* (SL1344) alone or in the presence of cytochalasin D or in the presence of Rac1 Inhibitor. (G) Effect of lipopolysaccharide (LPS) and other ligands on ELMO1-mediated TNF- $\alpha$  responses measured in J774, control, and ELMO1 shRNA cells after 3 hours of LPS treatment (500  $\mu$ g/mL). Data represent the mean  $\pm$  SD of three separate experiments. Data in C–G represent the mean  $\pm$  standard deviation of three separate experiments. \* $P \leq .05$ , two-tailed Student  $t$  test.

ELMO1 shRNA cells 15 minutes after *Salmonella* infection compared to the control shRNA cells (Figure 4A). The phosphorylation of p65 was reduced in ELMO1 shRNA cells compared to the control shRNA cells after 15 minutes and 30

minutes of *Salmonella* infection (see Figure 4A). The phosphorylation of p38 and phosphorylation of ERK<sub>1/2</sub> were lower in ELMO1 shRNA cells after infection compared with the total p38 and total ERK<sub>1/2</sub>, respectively (see Figure 4B).

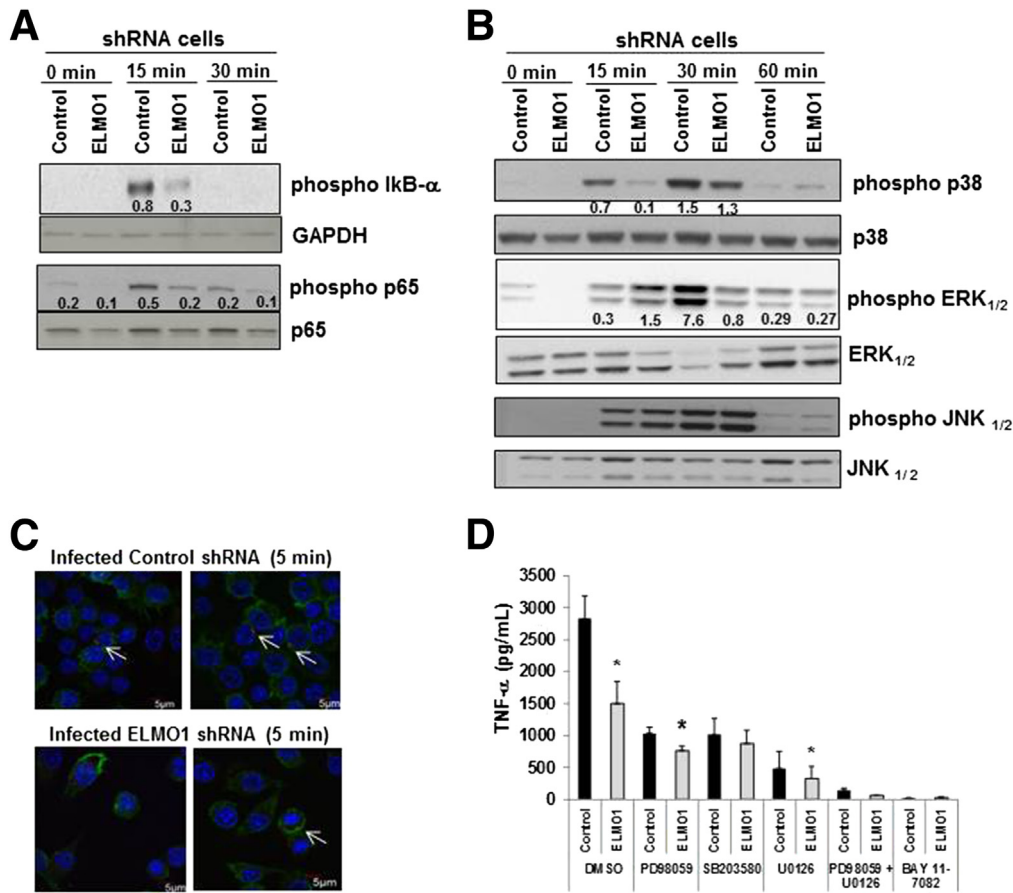


**Figure 4.** Engulfment and cell motility protein 1 (ELMO1)-mediated tumor necrosis factor- $\alpha$  (TNF- $\alpha$ ) responses are induced via the NF- $\kappa$ B and MAP kinase pathway. (A) Role of ELMO1 in nuclear factor  $\kappa$ B (NF- $\kappa$ B) activation evaluated in control and ELMO1 small-hairpin RNA (shRNA) cells by immunoblotting phospho-I $\kappa$ B and phospho p65 after *Salmonella* infection for the indicated time. The same blot was stripped and reprobed with antibodies to detect the glyceraldehyde-3-phosphate dehydrogenase (phosphorylating) (GAPDH) and total p65. (B) Control and ELMO1 shRNA cells incubated with *Salmonella* (SL1344) for indicated time points. Cells were harvested and lysed, and Western blots were performed with phospho-specific antibodies to detect p38 mitogen-activated protein kinase (MAPK), extracellular signal-regulated kinases 1/2 (ERK<sub>1/2</sub>), and c-Jun N-terminal kinase 1/2 (JNK<sub>1/2</sub>). A transient increase in p38 MAPK phosphorylation (15 minutes and 30 minutes) and ERK<sub>1/2</sub> (30 minutes) was observed in control cells compared with ELMO1 shRNA cells. The figures in A and B represent three independent experiments. (C) Bacterial internalization confirmed using confocal microscopy after infection of control and ELMO1 shRNA cells with SL1344-RFP (*red*) after 5 minutes of infection. The actin of the macrophages was stained with phalloidin (*green*), and the nuclei was stained with Hoechst (*blue*). (D) To investigate the effect of p38 MAPK and ERK<sub>1/2</sub> kinases, control and ELMO1 shRNA cells infected with *Salmonella* (SL1344) for 3 hours in the presence and absence of p38 MAPK inhibitor SB203580 (10  $\mu$ M), ERK<sub>1/2</sub> inhibitor PD98059 (50  $\mu$ M), and U0126 (10  $\mu$ M), and NF- $\kappa$ B inhibitor BAY 11-7082 (10  $\mu$ M). Subsequently, supernatants were assayed for TNF- $\alpha$  by enzyme-linked immunosorbent assay. Data represent the mean  $\pm$  standard deviation of three separate experiments. \* $P$   $\leq$  .05, compared with the respective control shRNA, two-tailed Student  $t$  test.

In contrast, phospho JNK levels were comparable in infected control and ELMO1 shRNA cells. To ensure the inflammatory signaling was triggered by internalized bacteria and not from their attachment to a membrane receptor, we used confocal microscopy to visualize control and ELMO1 shRNA cells 5 minutes after infection. The presence of internalized bacteria at early time points indicated that activation of signaling could be the consequence of internalization (see Figure 4C).

To examine the role of the MAP kinases and NF- $\kappa$ B signaling on TNF- $\alpha$  production, we infected with *Salmonella* cells treated with specific inhibitors or vehicle controls and

assessed them. PD98059 [2-(2-amino-3-methoxyphenyl)-4*H*-1-benzopyran-4-one] and U0126 [1,4-diamino-2,3-dicyano-1,4-bis(methylthio)butadiene], two inhibitors of ERK activation, as well as the p38 inhibitor SB203580 [4-(4-fluorophenyl)-2-(4-methylsulfinylphenyl)-5-(4-pyridyl)1*H*-imidazole], all reduced TNF- $\alpha$  to the levels detected in the control shRNA cells after 1 hour of infection (see Figure 4D). Interestingly, the NF- $\kappa$ B inhibitor that blocks phosphorylation of I $\kappa$ B $\alpha$  (BAY 11-7082 [(*E*)-3-(4-methylphenyl)sulfonylprop-2-enenitrile]) and the combination of ERK and p38 inhibitor blocked TNF- $\alpha$  production completely in the



control shRNA cells after infection. The production of TNF- $\alpha$  was undetectable in all treatments without infection (data not shown).

### **Bacterial Colonization, Dissemination, and Inflammation Are Regulated by ELMO1 In Vivo**

To determine the relevance of ELMO1 in vivo, the impact of ELMO1 on the pathogenesis of *Salmonella* infection was assessed in WT and ELMO1 KO mice without any prior antibiotic treatment. After oral infection, *Salmonella* translocate and disseminate to the spleen and liver,<sup>19</sup> so the approach used isolated the role of ELMO1 on host responses and bacterial burden from any effects of the antibiotics on the microbiota.

Five days after oral infection with *Salmonella* (SL1344), the bacterial load in the ileum and spleen was decreased in ELMO1 KO mice compared with WT littermates (Figure 5A). To assess the role of ELMO1 in regulating inflammatory responses in vivo, the expression of TNF- $\alpha$  mRNA was assessed by real-time RT-PCR in the ileum and spleen of infected WT mice and ELMO1 KO mice. Figure 5B shows the decreased TNF- $\alpha$  expression in the infected ileum and spleen of ELMO1 KO mice compared with the WT control.

As the cytokine array also implicated ELMO1 in the regulation of other cytokines, we assayed MCP-1 expression in the ileum and spleen of WT and ELMO1 KO mice. The real-time RT-PCR data showed reduced MCP-1 in the infected ileum and spleen of ELMO1 KO mice compared with the WT control (see Figure 5C). As infection induces the accumulation of inflammatory cells, leading to an increase in the size of an affected tissue, we measured the weight of the spleens from infected or uninfected WT and ELMO1 KO mice. The infected WT mice had enlarged spleens with an increased weight compared with the infected ELMO1 KO mice (see Figure 5D and E).

The *Salmonella* infection of the WT mice showed obvious inflammatory changes in the cecum, whereas these alterations were less severe in the ELMO1 KO mice (Figure 6A). To examine the effects on the cecum in more detail, we compared the weight of the cecum in age- and sex-matched WT and ELMO1 KO uninfected and infected mice. The infected ELMO1 KO mice ceca weighed more than the WT infected cecum (see Figure 6B). Further, the cecal histopathology after *Salmonella* infection showed reduced inflammatory cell infiltration, less submucosal edema, and less damage to a more normal-appearing epithelial architecture in the ELMO1 KO mice compared with the WT mice (see Figure 6C). To evaluate the role of ELMO1 in regulating inflammation in detail, a scoring system was developed to compare edema in the submucosa, the presence of neutrophils and crypt abscesses, and mononuclear infiltrates (Table 1). The histopathology revealed less severe inflammation in the ELMO1 KO mice compared with the infected WT mice (summary data in Figure 6D).

ELMO1 regulates MCP-1 expression, and this chemokine contributes to the recruitment of monocyte/macrophages. Therefore, cecal sections from WT and ELMO1 KO mice were stained to detect the macrophage marker F4/80

(see Figure 6E). Interestingly, the population of F4/80-positive macrophage and Gr-1-positive neutrophils were similar between the WT and ELMO1 KO mice without infection. The WT mice showed a higher number of recruited mononuclear cells than the ELMO1 KO mice, which correlated with a decrease in the expression of chemokines such as MCP-1. The histopathology of ileum after *Salmonella* infection showed reduced inflammatory cell infiltration and less damage to a more normal-appearing epithelial architecture in the ELMO1 KO mice compared with the WT mice (see Figure 6C).

### **ELMO1 Expression by Myeloid Cells Enables Cytokine Responses and the Dissemination of Salmonella**

During oral infection *Salmonella* enters through the ileum, spreads to mesenteric lymph nodes, and eventually (by day 5) spreads to the liver and spleen. Macrophages have an important role in dissemination of *Salmonella* to the liver and spleen, so we examined the bacterial dissemination and intestinal inflammation in myeloid cell specific (LysM-cre driven) ELMO1-deficient mice. Strikingly, the ileum and spleen of ELMO1<sup>fl/fl</sup> LysM cre positive mice showed a significant reduction in bacterial load (Figure 7A) and corresponding inflammation compared with the LysM cre negative controls (see Figure 7B). These results suggested that ELMO1 in the myeloid cells of ileum and spleen were responsible for *Salmonella* dissemination and proinflammatory responses.

## **Discussion**

The key finding in this study was the ELMO1-Rac1 dependence of proinflammatory cytokine induction by *Salmonella* after internalization into macrophages. This conclusion was based on the observation that impairing ELMO1/Rac expression and/or function significantly attenuated key signaling pathways, bacterial internalization, and TNF- $\alpha$  and MCP-1 production in response to infection. The physiologic relevance of ELMO1-mediated engulfment was demonstrated in intestinal macrophages isolated from ELMO1 KO mice. Moreover, ELMO1 KO mice had a reduced *Salmonella* burden and attenuated inflammatory responses in the ileum, spleen, and cecum, implicating this molecule in the pathogenesis of disease.

Several bacterial recognition receptors/adapters are important in initiating inflammation. TLR4 is a key Toll-like receptor involved in the control of *Salmonella* Typhimurium infection in mice where it can signal in a MyD88-independent fashion.<sup>20</sup> MyD88-deficient mice showed a reduction in the severity of the pathologic lesions in *Salmonella*-mediated colitis but still have inflammatory changes that indicate the involvement of a MyD88 independent pathway during *Salmonella* infection.<sup>11,21</sup> Other receptors, for example, Nod-like receptor, may play an essential role in host defense after infection with invasive pathogens.<sup>17,22</sup> These observations point to the redundancy in molecular sensors that plays an important role in regulating host responses. Although many receptors recognize

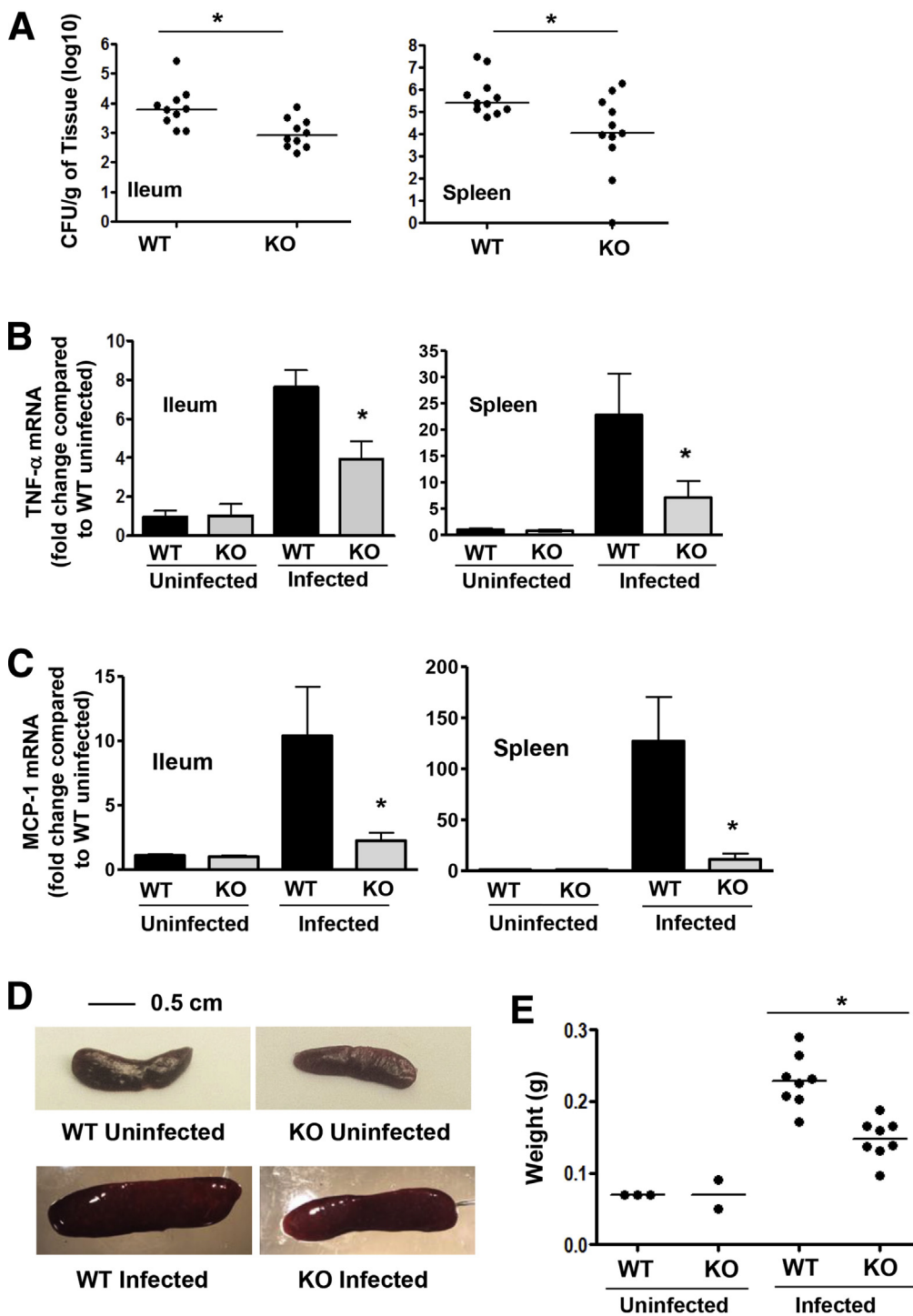


**Figure 5. Engulfment and cell motility protein 1 (ELMO1) regulates bacterial dissemination and inflammation in vivo.** (A) Bacterial burden assessed in the ileum and spleen of wild-type (WT) and ELMO1 knockout (KO) mice 5 days after *Salmonella* infection. (B) Real-time reverse-transcription polymerase chain reaction (RT-PCR) performed for tumor necrosis factor- $\alpha$  using RNA isolated from the ileum and spleen of uninfected and infected wild-type (WT) and ELMO1 KO mice 5 days after *Salmonella* infection. (C) Real-time RT-PCR performed for monocyte chemoattractant protein 1 (MCP-1) using RNA isolated from the ileum and spleen of uninfected and infected WT and ELMO1 KO mice 5 days after *Salmonella* infection. (D) Representative photomicrographs of spleen from uninfected and infected WT and ELMO1 KO mice captured using the same magnification. (E) Weights of spleens from age- and gender-matched groups of uninfected and infected WT and ELMO1 KO mice. In A and E the data represent the median and in B and C the median  $\pm$  standard error of the mean of 8–10 mice from three independent experiments. \* $P < .05$ , Mann-Whitney *U* test.

bacterial ligands and stimulate host responses, we suggest that these responses occur largely from within the cell after engulfment of the target, resulting in an amplified signal from the concentration of bacterial PAMPs within the phagosomes. In this study we show that the ELMO1/Rac pathway not only mediates the internalization of bacteria, but this internalization is essential for the inflammatory response induced by *Salmonella* infection.

In our previous report, we showed that BAI1 binds bacterial LPS expressed by *Salmonella* and *Escherichia coli*. After binding, BAI1 triggers engulfment by the ELMO1 pathway.<sup>4</sup> In an interesting report, Handa et al<sup>23</sup> showed that the *Shigella* effector protein IpgB1 interacts with ELMO1 and facilitates bacterial internalization. It is likely that the BAI1/ELMO1 pathway is used by several species of enteric bacteria, and future studies will further elucidate the mechanism.

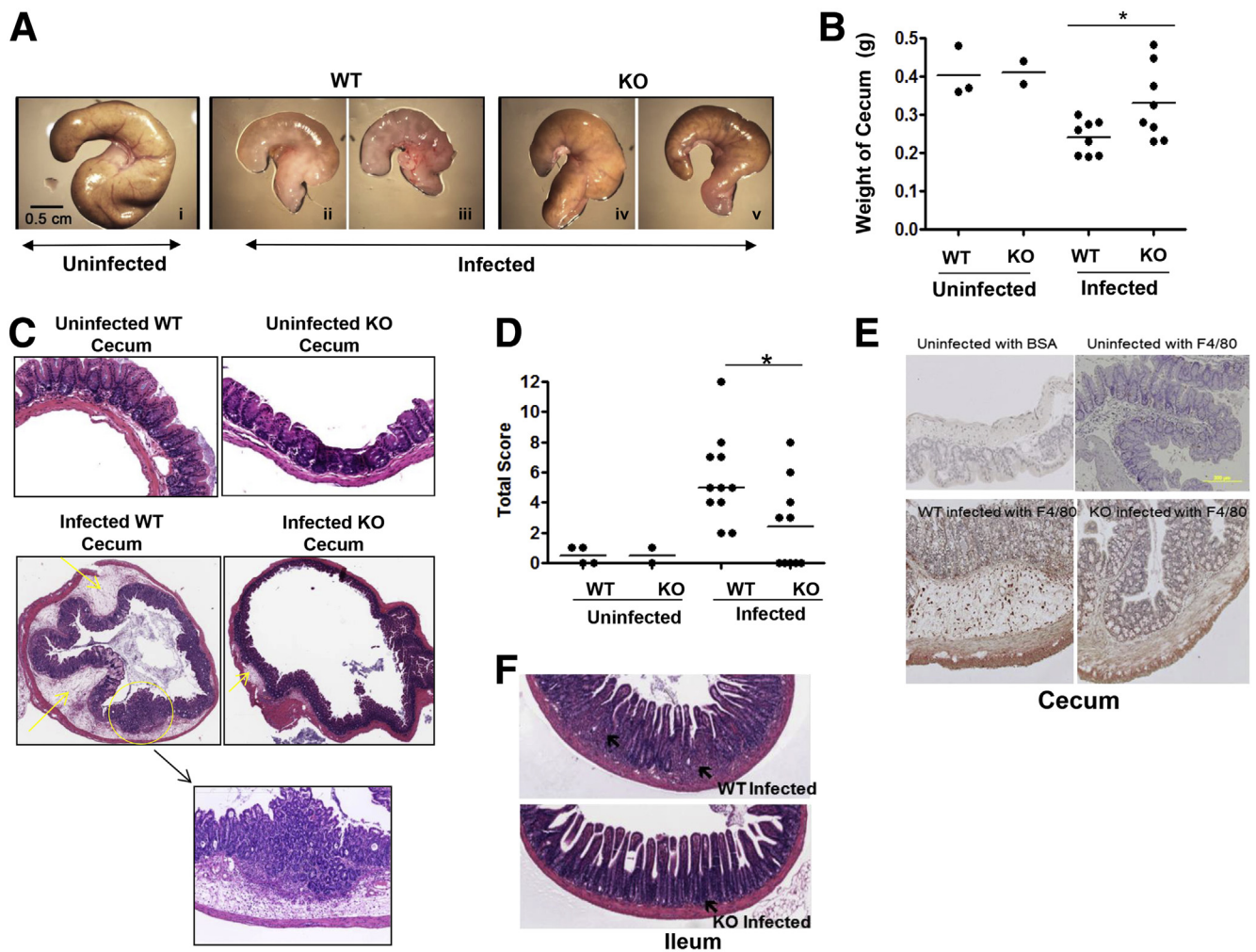


**Figure 6. The effect of engulfment and cell motility protein 1 (ELMO1) on cecal inflammation after *Salmonella* infection.** (A) Representative photomicrographs of ceca from uninfected and infected wild-type (WT) and ELMO1 knockout (KO) mice captured using the same magnification. (B) Cecum weight of uninfected and infected WT and ELMO1 KO mice. Data represent the median of 10 age- and gender-matched mice from three independent experiments. (C) Histology of H&E-stained cecal tissue from uninfected and infected WT and ELMO1 KO mice. Images were captured at identical magnification. A representative figure was selected from the three independent experiments. (D) Total inflammation score of uninfected and infected cecal tissue assessed in WT and the ELMO1 KO mice, as described in *Materials and Methods*. We used 10 infected WT and ELMO1 KO mice, and we compared them with the uninfected controls (4 WT and 2 KO). \* $P < .05$ , Mann-Whitney  $U$  test. (E) Immunohistochemistry of cecum with the F4/80 antibody to show the infiltration of macrophages after infection. (F) Histology of H&E stained ileum tissue from uninfected and infected WT and ELMO1 KO mice. Images were captured at identical magnification. A representative figure was selected from the three independent experiments.

The internalization of bacteria into cells is due to either bacterial-driven invasion or host cells mediating phagocytosis. SPI1 mediates invasion into epithelial cells, after which it transverse the epithelium through the SPI2-dependent trafficking pathway. Efficient internalization of multiple bacterial species<sup>24</sup> requires the involvement of the small Rho GTPases Rac1 and Cdc42, which are important for the organization of actin filaments and membrane extensions that facilitate phagocytosis. A previous report showed that the SPI1 effectors SopB and SopE promote *Salmonella* invasion into epithelial cells and intestinal inflammation by regulating Rho GTPases Rac1 and Cdc42.<sup>25</sup> Changes in Rho GTPases are sensed by Nod1, demonstrating another role

for Nod1 in regulating host responses<sup>7</sup>. However, most of these studies examined epithelial cells. During a natural infection, lamina propria mononuclear phagocytes engulf the infected epithelium or extracellular bacteria, providing an environment for further bacterial replication as well as dissemination throughout the host.<sup>26</sup> In contrast to epithelial cells, the ELMO1-mediated internalization into macrophages was SopB and SopE independent (data not shown). At this time, it is unclear which bacterial factors within the phagosome account for differences in the cytokine responses induced in macrophages.

Previously we showed that ELMO1 regulates the transcription of IL-33 mediated by Med-31.<sup>27</sup> To understand the



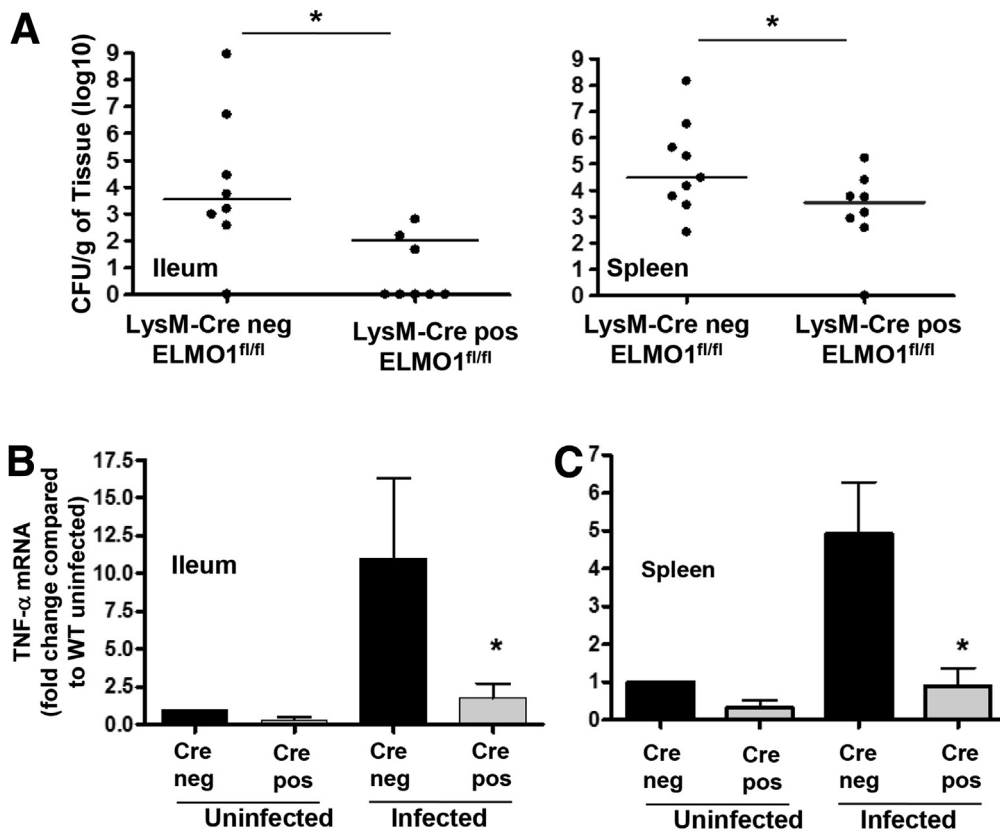


**Figure 7.** Myeloid cell-specific engulfment and cell motility protein 1 (ELMO1) is involved in *Salmonella* dissemination and inflammatory responses. (A) Bacterial burden assessed in the ileum and spleen of LysM cre negative ELMO1<sup>fl/fl</sup> and LysM cre positive ELMO1<sup>fl/fl</sup> mice 5 days after *Salmonella* infection. (B) Real-time reverse-transcription polymerase chain reaction performed for tumor necrosis factor- $\alpha$  using RNA isolated from the ileum and spleen of uninfected and infected LysM cre negative ELMO1<sup>fl/fl</sup> and LysM cre positive ELMO1<sup>fl/fl</sup> mice 5 days after *Salmonella* infection. In A the data represent the median, and in B data represent the median  $\pm$  the standard error of the mean of 8–10 mice from independent experiments. \* $P < .05$ , Mann-Whitney  $U$  test.

scope of ELMO1-mediated cytokine responses, we assayed an array of cytokines and chemokines in ELMO1 shRNA cells after *Salmonella* infection. We found MCP-1, TNF- $\alpha$ , keratinocyte-derived chemokine (KC), and RANTES were inhibited in ELMO1 shRNA cells (Figure 3B). Maximal cytokine responses may require internalization of the bacteria in view of the brief time that intact extracellular bacteria encounter surface PRRs. This notion is supported by the fact that bacteria were detected within the phagocytes as soon as 5 minutes after infection. Although the TNF- $\alpha$  responses induced by LPS in control and ELMO1 shRNA cells were comparable (Figure 3G), the cytochalasin D and Rac1 inhibitors that blocked *Salmonella* internalization reduced proinflammatory cytokine production significantly. Again, these observations favor the interpretation that the sensing of intracellular cues was compromised in ELMO1-deficient cells after exposure to intact bacteria.

One of the striking results from the study is that ELMO1 and Rac1 signaling are additive in terms of the cytokine generation after *Salmonella* infection compared as with the inhibition of ELMO1 alone, suggesting the existence of ELMO1-independent Rac1 activation. Whether any Nod-mediated bacterial sensing leads to inflammatory responses in macrophages will need to be addressed in future studies. It is expected that in the complex biological system, redundant pathways may allow a phagocyte to respond more efficiently. In addition, phagocytes from different tissues use different mechanisms for bacterial recognition and

engulfment. This conclusion was supported by our observation that bacterial internalization was abrogated in intestinal macrophages from ELMO1 KO mice.

Our present study shows that internalization was indispensable for cytokine production and that ELMO1 and Rac1 collectively were required for maximal internalization and proinflammatory responses. With these experimental approaches, the cytokine responses were attenuated, which may compromise potentially protective host defenses. However, the bacterial burden in cells or ELMO1 KO mice after infection with *Salmonella* was also lower. Although phagocytosis of pathogens is important for host defenses, it is possible that limiting bacterial internalization is ultimately more beneficial to the host than the attenuation in inflammatory mediators. However, the advantage to the host conferred by the decrease in immune-mediated tissue damage cannot be discounted. It was observed that ELMO1-KO mice appeared clinically more active after infection, which suggests that the net effect was beneficial. The ideal balance between host responses and immune-mediated damage likely involves multiple pathways, and ELMO1 is one such contributing factor.

Previous studies showed the involvement of ELMO1/Dock180 in Rac-mediated cell migration.<sup>28</sup> To rule out cell migration as the cause of the inflammatory responses, we found no significant differences in the population of F4/80 positive macrophage and Gr-1 positive neutrophils when comparing WT and ELMO1 KO mice without any



infection (data not shown). However, after infection, inflammatory cell infiltrates and F4/80 positive macrophages were less abundant in ELMO1 KO mice compared with the WT mice (see Figure 6E), presumably owing to the decrease in chemokine production. Importantly, intestinal macrophages isolated from ELMO1 KO mice failed to internalize *Salmonella* whereas infection of these mice led to a lower bacterial load in the ileum and spleen and attenuated TNF- $\alpha$  and MCP-1 responses compared with WT mice.

Together, these findings suggest that ELMO1 plays an essential role in the pathogenesis of enteric infections with *Salmonella* Typhimurium. Future studies are needed to understand whether ELMO1 can differentially regulate immune response after sensing pathogens and commensals to predict the pathogenicity of an infection.

## References

1. Broz P, Ohlson MB, Monack DM. Innate immune response to *Salmonella* typhimurium, a model enteric pathogen. *Gut Microbes* 2012;3:62–70.
2. Hallstrom K, McCormick BA. *Salmonella* interaction with and passage through the intestinal mucosa: through the lens of the organism. *Front Microbiol* 2011;2:88.
3. Nish S, Medzhitov R. Host defense pathways: role of redundancy and compensation in infectious disease phenotypes. *Immunity* 2011;34:629–636.
4. Das S, Owen KA, Ly KT, et al. Brain angiogenesis inhibitor 1 (BAI1) is a pattern recognition receptor that mediates macrophage binding and engulfment of Gram-negative bacteria. *Proc Natl Acad Sci USA* 2011;108:2136–2141.
5. Park D, Tosello-Trampont AC, Elliott MR, et al. BAI1 is an engulfment receptor for apoptotic cells upstream of the ELMO/Dock180/Rac module. *Nature* 2007;450:430–434.
6. Gumienny TL, Brugnera E, Tosello-Trampont AC, et al. CED-12/ELMO, a novel member of the CrkII/Dock180/Rac pathway, is required for phagocytosis and cell migration. *Cell* 2001;107:27–41.
7. Keestra AM, Winter MG, Auburger JJ, et al. Manipulation of small Rho GTPases is a pathogen-induced process detected by NOD1. *Nature* 2013;496:233–237.
8. Lee CA, Falkow S. The ability of *Salmonella* to enter mammalian cells is affected by bacterial growth state. *Proc Natl Acad Sci USA* 1990;87:4304–4308.
9. Elliott MR, Zheng S, Park D, et al. Unexpected requirement for ELMO1 in clearance of apoptotic germ cells in vivo. *Nature* 2010;467:333–337.
10. Nava P, Koch S, Laukoetter MG, et al. Interferon-gamma regulates intestinal epithelial homeostasis through converging beta-catenin signaling pathways. *Immunity* 2010;32:392–402.
11. Coburn B, Li Y, Owen D, et al. *Salmonella enterica* serovar Typhimurium pathogenicity island 2 is necessary for complete virulence in a mouse model of infectious enterocolitis. *Infect Immun* 2005;73:3219–3227.
12. Livak KJ, Schmittgen TD. Analysis of relative gene expression data using real-time quantitative PCR and the  $2^{-\Delta\Delta CT}$  method. *Methods* 2001;25:402–408.
13. Islam AF, Moss ND, Dai Y, et al. Lipopolysaccharide-induced biliary factors enhance invasion of *Salmonella* enteritidis in a rat model. *Infect Immun* 2000;68:1–5.
14. Mastroeni P, Villarreal-Ramos B, Hormaeche CE. Effect of late administration of anti-TNF alpha antibodies on a *Salmonella* infection in the mouse model. *Microb Pathog* 1993;14:473–480.
15. Nakano Y, Kasahara T, Mukaida N, et al. Protection against lethal bacterial infection in mice by monocyte-chemotactic and -activating factor. *Infect Immun* 1994;62:377–383.
16. Depaolo RW, Lathan R, Rollins BJ, et al. The chemokine CCL2 is required for control of murine gastric *Salmonella enterica* infection. *Infect Immun* 2005;73:6514–6522.
17. Arthur JS, Ley SC. Mitogen-activated protein kinases in innate immunity. *Nat Rev Immunol* 2013;13:679–692.
18. Vallabhapurapu S, Karin M. Regulation and function of NF- $\kappa$ B transcription factors in the immune system. *Annu Rev Immunol* 2009;27:693–733.
19. Watson KG, Holden DW. Dynamics of growth and dissemination of *Salmonella* in vivo. *Cell Microbiol* 2010;12:1389–1397.
20. Barton GM, Medzhitov R. Toll-like receptor signaling pathways. *Science* 2003;300:1524–1525.
21. Keestra AM, Godinez I, Xavier MN, et al. Early MyD88-dependent induction of interleukin-17A expression during *Salmonella* colitis. *Infect Immun* 2011;79:3131–3140.
22. Robertson SJ, Girardin SE. Nod-like receptors in intestinal host defense: controlling pathogens, the microbiota, or both? *Curr Opin Gastroenterol* 2013;29:15–22.
23. Handa Y, Suzuki M, Ohya K, et al. Shigella IpgB1 promotes bacterial entry through the ELMO-Dock180 machinery. *Nat Cell Biol* 2007;9:121–128.
24. Wong KW, Isberg RR. Emerging views on integrin signaling via Rac1 during invasin-promoted bacterial uptake. *Curr Opin Microbiol* 2005;8:4–9.
25. Hardt WD, Chen LM, Schuebel KE, et al. *S. typhimurium* encodes an activator of Rho GTPases that induces membrane ruffling and nuclear responses in host cells. *Cell* 1998;93:815–826.
26. Muller AJ, Kaiser P, Dittmar KE, et al. *Salmonella* gut invasion involves TTSS-2-dependent epithelial traversal, basolateral exit, and uptake by epithelium-sampling lamina propria phagocytes. *Cell Host Microbe* 2012;11:19–32.
27. Mauldin JP, Lu M, Das S, et al. A link between the cytoplasmic engulfment protein Elmo1 and the Mediator complex subunit Med31. *Curr Biol* 2013;23:162–167.
28. Grimsley CM, Kinchen JM, Tosello-Trampont AC, et al. Dock180 and ELMO1 proteins cooperate to promote evolutionarily conserved Rac-dependent cell migration. *J Biol Chem* 2004;279:6087–6097.
29. Wilson JM, Kurtz CC, Black SG, et al. The A2B adenosine receptor promotes Th17 differentiation via stimulation of dendritic cell IL-6. *J Immunol* 2011;186:6746–6752.

---

Received January 19, 2015. Accepted February 19, 2015.

**Correspondence**

Address correspondence to: Peter B. Ernst, DVM, PhD, University of California San Diego, Division of Comparative Pathology and Medicine, Department of Pathology, MC 0063, San Diego, California 92093-0063. e-mail: [pernst@ucsd.edu](mailto:pernst@ucsd.edu); fax: 858.246.0523.

**Acknowledgments**

The authors thank Bobbie Gomez, Adrienne B. Horner, Courtney L. Lyons, and Rama F. Pranadinata for mice genotyping and RNA isolation. The imaging

facility was supported by the UCSD Cancer Center Specialized Support Grant P30 CA23100.

**Conflicts of interest**

The authors disclose no conflicts.

**Funding**

This study was funded by National Institutes of Health grants AI079145, DK084063, and AI070491 (to P.B.E.) and UCSD Academic Senate seed money UCSD RM089H-DAS and National Institutes of Health grants DK099275 (to S.D.).